

Heterologous expression of moss LHCSR1: the Chlorophyll a-xanthophyll pigment-protein complex catalyzing Non-Photochemical Quenching, in *Nicotiana sp.*

Alberta Pinnola, Leonardo Ghin, Elisa Gecchele, Matilde Merlin, Alessandro Alboresi, Linda Avesani, Mario Pezzotti, Stefano Capaldi, Stefano Cazzaniga and Roberto Bassi

From Department of Biotechnology, University of Verona, Strada Le Grazie 15, 37134 Verona, Italy

Running title: Heterologous expression of LHCSR1

To whom correspondence should be addressed: Roberto Bassi, Dept. of Biotechnology, University of Verona, Strada Le Grazie 15, 37134 Verona, Italy. Tel.: Phone: 39-45-802-7916; Fax: 39-45-802-7035; E-mail: roberto.bassi@univr.it

Keywords: photosynthesis, *P. patens*, tobacco, stable transformation, transient transformation, heterologous expression, LHC, LHCSR protein, NPQ.

CAPSULA

Background: LHCSR protein in algae and mosses is essential for NPQ.

Results: Expression and characterization of *Physcomitrella patens* LHCSR1 protein upon heterologous expression in *N. benthamiana* and *N. tabacum* was obtained.

Conclusion: LHCSR1 is the first member of LHC protein family lacking Chlorophyll *b*. It is active in NPQ.

Significance: LHCSR1 isolation is crucial for the elucidation of the NPQ mechanism.

ABSTRACT

Oxygenic photosynthetic organisms evolved mechanisms for thermal dissipation of energy absorbed in excess to prevent formation of reactive oxygen species. The major and fastest component, called Non-Photochemical Quenching, occurs within Photosystem II antenna system by the action of two essential LHC-like proteins: PSBS in plants and LHCSR in green algae and diatoms. In the evolutionary intermediate *Physcomitrella patens*, a moss, both gene products are active. These proteins, present in low amounts, are difficult to purify, preventing structural and functional analysis. Here, we report on the overexpression of the LHCSR1 protein from *P. patens* in the heterologous systems, *Nicotiana benthamiana* and *Nicotiana tabacum*, using transient and stable nuclear transformation. We show that the protein accumulated in both heterologous systems is in its mature form, localizes in the chloroplast thylakoid membranes and is

correctly folded with Chlorophyll *a* and xanthophylls but without Chlorophyll *b*, an essential chromophore for plants and algal LHC proteins. Finally, we show that recombinant LHCSR1 is active in quenching *in vivo* implying the recombinant protein obtained is a good material for future structural and functional studies.

INTRODUCTION

Photosynthesis depends on light and yet excess light can be harmful for the photosynthetic apparatus when its intensity exceeds the activity of the photosynthetic electron transport chain. Indeed, light in excess with respect to the photochemical quenching activity, increases lifetime of chlorophyll singlet excited states ($^1\text{Chl}^*$) thus increasing the probability of triplet chlorophyll ($^3\text{Chl}^*$) formation. Long living triplets react with O_2 to yield singlet oxygen ($^1\text{O}_2$), leading to photodamage and photoinhibition (1–3). Plants developed multiple photoprotection mechanisms against photooxidation. A major mechanism for response to changes in light availability is Non-Photochemical Quenching (NPQ), which is activated upon exposure to excess light and leads to the dissipation of excess energy absorbed as heat (4, 5). NPQ includes several components whose relative importance for photoprotection depends on species and physiological state: the energy quenching (qE), is reversibly activated within seconds upon an increase in light

intensity and has the highest potential for quenching. Slowly-relaxing components are comprised under the definition of “inhibitory quenching” (qI), activated within several minutes of excess irradiance and relaxing within 1–2 h in the dark (5–7). qI includes qZ, caused by binding of zeaxanthin to Light Harvesting Complexes (LHC) antenna proteins, decreasing their fluorescence yield. Zeaxanthin is produced in excess light from pre-existing violaxanthin and is photoprotective (8). Finally, the actual quenching from photoinhibition (9), which is relaxed upon repair of photodamaged Photosystem II (PSII) (10). An intermediate kinetic component, qM, relaxing in 8–20 minutes has been attributed to the chloroplast avoidance relocation in the cell, implying this fluorescence decay is not depending on quenching (11). Among quenching mechanisms, the most studied and yet obscure is qE, whose mechanistic details are still matter of intense debate some 50 years after its first report (12). Forward genetic analysis showed qE requires one of two *lh*c-like gene products, PSBS and LHCSR, respectively in plants and algae. These are essential for sensing pH of thylakoid lumen (13, 14) and transduction into quenching events. While PSBS is not a typical pigment-binding protein (15, 16) making it unlikely as a site for quenching reactions which have been reported to occur in interacting LHC proteins (17–19), LHCSR does bind Chl and xanthophylls (20). In *P. patens*, LHCSR is responsible for most of quenching activity (21) which is strongly enhanced by zeaxanthin binding (22), making LHCSR the ideal system for structure-functional studies aimed at elucidating the properties of this molecular switch which regulates the photon use efficiency in unicellular algae and mosses resuming the two functions of pH detection and quenching of the chlorophyll excited states (14, 20). However, the level of LHCSR is low in thylakoids and has physico-chemical properties similar to the highly abundant LHCs, which has so far hampered purification. Heterologous expression systems have been exploited to obtain a recombinant protein, for refolding *in vitro* with pigments in a second stage (20, 23) and yet this method is expensive and did not allow successful crystallization (Chang, Liu, Ballottari and Bassi, unpublished results). With the aim of scaling up production of this gene product, we attempted heterologous expression

in two *Nicotiana* species, which proved to be a useful system, yielding LHCSR as a pigment-protein whose properties are consistent with previous reports. Also, we show that LHCSR is active in quenching *in vivo*, suggesting that the recombinant product obtained closely features the protein responsible for NPQ in mosses, therefore providing a solid basis for future structural and functional studies.

EXPERIMENTAL PROCEDURES

Construction of plant expression vector-cDNA obtained from *P. patens* protonema grown in control conditions was used as starting material. Coding sequence for LHCSR1 (XM_001776900.1) with and without the HisTag were amplified by PCR and used as a template to construct the pENTR™/D-TOPO based vectors. The following primers were used: forward primer 5'-CACCTCGCTCTGCAACTTTCCTTT-3' for both the constructs, the reverse primer for LHCSR1 without HisTag 5'-GGGGACCACTTTGTACAAGAAAGCTGGGTCGACTGCGAATCAATCAGAA and the reverse primer for LHCSR1 HisTag 5'-TCAGTGGTGGTGATGATGATGGCTGCCGCGCGGCACCAGCAGGCCCAATCTCTTGAACAA-3'. The pENTR.LHCSR1 and pENTR.LHCSR1 HisTag vectors obtained were used for LR recombination reactions with the GATEWAY destination vector pK7WG2 (24), generating the final vectors pK7WG2.LHCSR1 and pK7WG2.LHCSR1 HisTag. The two vectors were transformed in *A. tumefaciens* EHA105 strain.

***N. tabacum* leaf transformation**-Tobacco (*Nicotiana tabacum* cv Petit Havana SR1) leaf disks were transformed with pK7WG2-based constructs as described (25). Kanamycin-resistant transgenic lines were selected and tested by immunoblot analysis using home-made polyclonal α -PpLHCSR antibody.

Agro-infiltration of *N. benthamiana* leaves-Bacterial suspension in infiltration buffer (10 mM MES, 10 mM MgCl₂, 100 μ M acetosyringone, pH 5.6), at a final O.D.₆₀₀=0.8, was used for syringe infiltration of 5–6 weeks-old *N. benthamiana* plants, 5 leaves were infiltrated for each plants and for each construct.

The recombinant protein time-course accumulation of PpLHCSR1 protein has been estimated by immunoblotting on total protein extract starting from disk of infected leaves collected for 7 days after agro-infiltration and grinded in Loading Buffer (LB) (62.5 mM Tris pH 6.8, 10% glycerol, 2% SDS and 3% β -mercaptoethanol).

Thylakoid extraction and pigment binding complex purification-Thylakoids were purified from *N. tabacum* and *N. benthamiana* leaves following a protocol for seed plants (26).

For separation of pigment binding complex, 500 μ g of thylakoid membranes were washed with 5 mM EDTA and resuspended at a final concentration of 1 mg/ml in 10 mM Hepes, pH 7.5. Samples were then solubilized at a final concentration of 0.5 mg/ml adding 1.6% n-Dodecyl- α -D-Maltopyranoside (α -DM) and 10 mM Hepes, pH 7.5 and vortexing for 1 min. After 10 min of ice incubation, thylakoid membranes were centrifuged at 15000X g for 10 min to eliminate unsolubilized material. Fractionation occurred upon ultracentrifugation on a 0.1 to 1 M sucrose gradient containing 0.03% α -DM and 10 mM Hepes, pH 7.5 (22 hours at 280000Xg and 4°C).

Deriphat PAGE-Non-denaturing Deriphat-PAGE was performed according to (27) with minor modifications. The stacking and the resolving gels contained respectively 3.5% (w/v) and 7% (w/v) acrylamide (38:1 acrylamide/bisacrylamide). Thylakoids, concentrated at 1 mg/ml of Chl, were solubilized with 0.8% α -DM. 500 μ g of Chl were loaded in each wide well for comparing LHCSR1 expressing plants (oeLHCSR1) to the corresponding wild-type (WT).

Nickel affinity chromatography-30 mg of Chl of thylakoid membranes from oeLHCSR1 with Histidine tail expressing plants (oeLHCSR1 HisTag) were washed with 5 mM EDTA and resuspended at a final concentration of 1 mg/ml in 10 mM Hepes, pH 7.5. Samples were then solubilized with 1% α -DM and then centrifuged at 15000Xg for 10 min to eliminate unsolubilized material. The supernatant was loaded onto a nickel affinity column equilibrated with the same buffer and the resin was washed with 2-3 column volumes of washing buffer (10

mM Hepes pH 7.5, 0.15 M NaCl, 10 mM imidazole, 0.03% α -DM). Further step-elutions were performed by increasing the imidazole concentration (25, 50 and 250 mM).

Pigment composition-The pigment composition of the complexes was analyzed by fitting the spectrum of the 80% acetone extracted pigments with the spectra of the individual pigments in acetone and by HPLC, as described previously (28, 29).

Absorption spectroscopy-Samples collected from the sucrose gradients were analysed by absorption spectroscopy using a SLM-Aminco DW-2000 (Aminco) spectrophotometer at room temperature. Spectra were also collected for native Chl-binding complexes after extraction from the acrylamide gel by grinding the slices in a buffer containing 10 mM HEPES, pH 7.5, and 0.03% α -DM.

SDS-PAGE and immunoblotting analysis-SDS-PAGE analyses were performed as described by (30). An acrylamide/bisacrylamide ratio of 75:1 and a total concentration of acrylamide of 4.5 and 15% were used respectively, for stacking and running gel. Urea (6 M) was also added into the running gel. Polypeptides, following SDS-PAGE, were transferred onto an Immobilon PVDF membrane (Millipore) using a Mini Trans-Blot cell (Bio-Rad) and detected by home-made polyclonal antibodies.

NPQ measurements-*In vivo* Chl fluorescence of *N. tabacum* leaf disks of WT and oeLHCSR1 plants was measured at room temperature on Fluorcam imaging fluorometers (Photon system instrument), with saturating light at 4000 μ mol m⁻²s⁻¹ and actinic light at 1200 μ mol m⁻²s⁻¹. Before measurements, plants were dark-adapted for 40 min at room temperature. Parameters F_v/F_m and NPQ were calculated as $(F_m - F_o)/F_m$ and $(F_m - F_{m'})/F_{m'}$ (31). Data are presented as means \pm SD of at least three independent experiments.

RESULTS

Expression of P. patens LHCSR1 in N. benthamiana and N. tabacum plants-The full length ORFs of LHCSR1 with or without Thrombin cleavable Histidine tail (HisTag) at the C-term of the protein were introduced by LR recombination into the binary GATEWAY

vector pK7WG2, under the control of the constitutive CaMV 35S promoter.

The resulting vectors, named pK7WG2.LHCSR1 and pK7WG2.LHCSR1 HisTag were used for stable (25) and transient (32, 33) *A. tumefaciens* mediated transformation of plants.

N. benthamiana was used as host for transient expression (34): five leaves of 5-6 week-old plants were agro-infiltrated. Upon infection, a time-course analysis was performed by collecting leaf disks for 7 days post-agro-infiltration (dpi) to identify the peak of recombinant protein accumulation. Total proteins were analyzed by SDS-PAGE and immunoblot with an α -PpLHCSR1 polyclonal antibody. α -CP43, a subunit of PSII core, was used as loading control. Figure 1 shows the time-course analysis of PpLHCSR1 (Fig. 1A) and PpLHCSR1 HisTag (Fig. 1B) expression in *N. benthamiana*. α -PpLHCSR1 antibody revealed a band at ~23 KDa apparent molecular weight (MW) in *N. benthamiana* leaf disks while 2 bands were detected in wild type (WT) *P. patens* sample, which contains both LHCSR1 and LHCSR2 (21). The LHCSR1 signal had the same apparent MW in both *N. benthamiana* and *P. patens*, implying the maturation of the precursor recombinant protein in *N. benthamiana* occurred as in the homologous moss system. In the case of oeLHCSR1 HisTag *N. benthamiana* plants, the MW of LHCSR1 is slightly higher respect to *P. patens* LHCSR1. This difference is due to the presence of the Thrombin cleavable Histidine tail affecting the mobility of the protein in SDS-PAGE gel. No reaction was observed in the untransformed WT *N. benthamiana* sample. In Fig. 1C & D, the accumulation of PpLHCSR1 with and without HisTag is shown. In both the constructs the protein was detectable at 2dpi and reached the maximum at 4 dpi.

Alternatively, we used *N. tabacum* cv Petit Havana SR1 for stable transformation into the nuclear genome. Transgenic plants were generated by agrobacterium-mediated transformation of leaf disks and *in vitro* regeneration of plants under Kanamycin selection. About 80 regenerated plants were analysed for each construct. Fig. 1E shows the accumulation of PpLHCSR1 protein by

immunoblotting analysis in oeLHCSR1 plants of *N. tabacum*. Similar to results with *N. benthamiana*, the reaction in the WT moss had the same apparent MW as the recombinant PpLHCSR1. PpLHCSR1 protein from oeLHCSR1 HisTag plants showed slightly slower migration than LHCSR1 from oeLHCSR1-expressing plants due to additional sequence encoding the tag and Thrombin target site (Fig.1F). The protein accumulation levels varied significantly between independently-transformed lines, likely reflecting the positional effects of random insertion (35). The protein level was used to select T1 transgenic lines (elite lines) for a breeding program to reach the homozygosis of the inserted transgene/s, which was initiated by self-crossing the best-performing T1 oeLHCSR1 and oeLHCSR1 HisTag transgenic plants. In the following paragraphs, the results obtained with T1 plants are reported.

Sub-cellular localization of LHCSR1 in thylakoid membranes and aggregation state analysis- The intracellular localization of recombinant PpLHCSR1 was analysed in *N. benthamiana* and *N. tabacum* plants. In mosses, LHCSR1 is encoded by the nuclear genome, translated in the cytoplasm and targeted towards the chloroplast (36). The transit-peptide is then removed and the apoprotein co-insertionally assembles in the thylakoid membranes with Chl and carotenoids (37). In order to study the intracellular fate of the recombinant protein in *Nicotiana* sp., thylakoid membranes were purified from *N. benthamiana* infected leaves 4 dpi and *N. tabacum* transgenic plants. Fig. 1G shows the results of immunoblotting analysis on thylakoid membranes using α -PpLHCSR antibody. LHCSR1 and LHCSR1 HisTag recombinant proteins were detected in thylakoids of both *N. benthamiana* and *N. tabacum* as well as in thylakoids from WT of *P. patens* but not in WT thylakoids of *N. benthamiana* and *N. tabacum* as well as in *lhcsr* Knock Out (KO) of *P. patens*, implying *Nicotiana* sp. machinery is competent for the targeting of PpLHCSR1 into the thylakoid compartment.

Next, we tested the aggregation state of recombinant tobacco-produced PpLHCSR1 as compared to the native *P. patens* LHCSR1 (22). Thylakoids were solubilized with the mild detergent α -DM and loaded onto a sucrose

gradient which was centrifuged at 280000Xg for ~22h. The separation pattern, consisting of 7 green bands, was similar in WT and oeLHCSR1 *N. benthamiana* or *N. tabacum* plants. Bands were collected from the gradient and analyzed by absorption spectroscopy and SDS-PAGE to identify their pigment-protein content and polypeptide composition. Fig. 2A shows the result of the sucrose gradient: in the upper part of the gradient, a yellow top band contained carotenoid-enriched free pigments (B1), monomeric LHCs (B2), trimeric LHCII (B3) and LHCII-CP29-CP24 complex (B4). In the central part of the gradient PSII core complex was found (B5) while in the lower part of the gradient migrated PSI-LHCI (B6) and PSII-LHCII supercomplexes (B7). The separation pattern was very similar in WT vs oeLHCSR1. Absorption spectra of B1 and B2 of oeLHCSR1 showed a Qy absorption peak red-shifted when compared with the corresponding fractions from WT (Fig. 3A-D); since a red-shifted spectrum is a typical characteristic of LHCSR1 protein (20, 22), this suggests LHCSR1 migrates in the region of B1 with monomeric LHCs. This characteristic was more evident in the case of *N. benthamiana* (Fig. 3A) where the Qy peak of B1 was shifted from 672.2 nm in WT to 677.7 nm in oeLHCSR1, while was less evident in *N. tabacum* plants (Fig. 3B). Absorption spectra of B2 also showed a small red shift of the Qy peak from 676.6 nm in WT to 677.7 nm in oeLHCSR1 of *N. benthamiana*, while was almost absent in the case of *N. tabacum* (Fig. 3C and D). No differences were found between the absorption spectra of WT and oeLHCSR1 of other bands (data not shown).

Further assessment of protein distribution was performed by SDS-PAGE: for each band, an equal volume was loaded onto the gel and the protein profile analyzed after Coomassie-blue staining (Fig. 2B). A clear signal of ~23 KDa was found in monomeric LHCs (B2) of *N. tabacum* oeLHCSR1 as well as in free pigments (B1) and monomeric LHCs (B2) of *N. benthamiana* oeLHCSR1 but absent in the samples from WT. Immunoblotting analysis confirmed that the Coomassie-stained 23 KDa band was indeed LHCSR1 (Fig. 2C).

Expression and purification of PpLHCSR1 HisTag by affinity chromatography-When *Nicotiana sp.* plants expressing the PpLHCSR1

HisTag version were analysed, a far lower accumulation level than PpLHCSR1 version was observed on a Chl basis (see below). Nevertheless, we attempted the purification of the recombinant protein by Ni-ion affinity chromatography. To this aim, thylakoid membranes purified from full grown tobacco leaves (about 30 mg Chl) were solubilized with α -DM and loaded onto a Nickel-chelating sepharose, followed by step elution with 25, 50 and 250 mM imidazole, respectively. The absorption spectrum of solubilized thylakoids showed two peaks at around 470 and 650 nm which are typical of Chl *b*, while that of the fraction eluted with 250 mM imidazole did not, implying a depletion in Chl *b* (Fig. 4A). SDS-PAGE analysis showed a major Coomassie-stained band at ~25 KDa MW, which was recognized by antibodies directed against HisTag (data not shown) and α -PpLHCSR (Fig. 4B), suggesting an enrichment in LHCSR1, with traces of high MW contaminants. In order to eliminate these contaminants and the possible free pigments, the fraction eluted with 250 mM imidazole was concentrated to 300 μ l and loaded onto a sucrose gradient which was run into a SW60 rotor overnight at 360000Xg, yielding the pattern shown in Fig. 4C consisting into a faint yellowish upper band (B1) and a lower green band (B2), a green pellet (P) was also observed. SDS-PAGE analysis of the fractions showed a single band, ~25 KDa, in B2 and multiple bands in P including a prominent ~25KDa component. The absorption spectrum of the green B2 band, obtained from sucrose gradient, was characterized by major peaks at 435 nm and 679.1 nm, respectively in the Soret and the Qy range and minor peaks at 488 nm and 628 nm while deeps were detected at 470 and 650 nm, the typical absorption wavelengths for Chl *b* in LHC proteins (38), implying that the recombinant protein bound mainly Chl *a* and carotenoids and is depleted of Chl *b*.

Recombinant LHCSR1 expression level- The abundance of the two recombinant proteins in the thylakoid fraction of both expression systems was determined by immuno-titration (Fig. 5A & B). For this aim, we used PpLHCSR1 HisTag, purified from *N. tabacum*, as a reference (Fig. 4C). A SDS-PAGE gel was loaded with serial dilutions of PpLHCSR1 HisTag (0.012, 0.025 and 0.05 μ g of Chl) and different amounts of

oeLHCSR1 thylakoids (0.12, 0.25, 0.5 and 0.75 μg of Chl) from both *N. benthamiana* and *N. tabacum*. The intensity of the immunoreaction was not dependent on whether the determination was performed with recombinant LHCSR1 alone or mixed to WT thylakoids. The reactivity of α -LHCSR antibody was evaluated by densitometric analysis of immunoreactions. We calculated that in 1 mg of Chl of thylakoids was present PpLHCSR1 protein corresponding to 0.13 ± 0.025 and 0.036 ± 0.002 mg of Chl in *N. benthamiana* and *N. tabacum* respectively (Fig. 5A). Similarly, we determined the abundance of recombinant LHCSR1 HisTag in thylakoids obtained both from agro-infiltrated *N. benthamiana* and stable transformed *N. tabacum* plants. In this case, the resulting yields were of 0.021 ± 0.001 and 0.011 ± 0.003 mg of recombinant protein per mg of Chl in *N. benthamiana* and *N. tabacum*, respectively (Fig. 5B).

Purification of untagged PpLHCSR1 using Deriphat-PAGE—Untagged PpLHCSR1 version accumulated higher levels of LHCSR1 protein respect to its tagged version in both *N. tabacum* and *N. benthamiana* (Fig. 5A & B). In order to attempt purification, non-denaturing Deriphat-PAGE was applied to fractionate low molecular mass proteins with high-resolution. Fig. 6 shows such a green gel of pigment-binding complexes from thylakoids of WT and oeLHCSR1 of *N. benthamiana* (Fig. 6A) and *N. tabacum* (Fig. 6B) after solubilization with 0.8% α -DM. In *N. benthamiana*, a well distinct additional green band migrating below the monomeric LHCs band, was present in oeLHCSR1 plants while absent in WT sample (Fig. 6A). In the case of transgenic *N. tabacum*, a clear distinguishable band corresponding to recombinant LHCSR1 was less visible, but the monomeric LHCs green band extended toward lower molecular mass when compared to the WT sample (Fig. 6B). The middle section of the gel including both samples was blotted into a polyvinylidene fluoride (PVDF) membrane and the migration of the PpLHCSR1 protein was detected with an α -PpLHCSR antibody. A clear reaction, in the oeLHCSR1 plants but not in the WT, was detectable at the apparent molecular weight corresponding to the low molecular weight green band, suggesting that non-denaturing Deriphat-

PAGE was effective in separating PpLHCSR1 from monomeric LHCs. Another clear reaction was also present in between monomers and trimers in the sample from oeLHCSR1 plants, suggesting the presence of a dimeric form for the protein. The remaining part of the gel was used for detailed fractionation: to this aim, the 20- to 100-KDa molecular mass range, including monomeric LHCs and trimers, was cut into thin slices that were eluted in a buffer solution containing 0.03% α -DM and 10 mM Hepes, pH 7.5. The eluate from each slice was submitted to HPLC pigment analysis, SDS-PAGE/immunoblotting (Fig. 6C & D) and absorption spectroscopy (Fig. 7).

Coomassie-blue staining showed that slices number 5, 6 and 7 from *N. benthamiana* and *N. tabacum* (Fig. 6C & D, respectively), corresponding to the green band observed in the Deriphat-PAGE, were strongly enriched in a polypeptide of apparent molecular weight of ~ 23 KDa which was absent in the corresponding sections from gel loaded with WT thylakoids and was reactive to α -PpLHCSR antibody.

In addition, based on immunoblot analysis upon Deriphat-PAGE, an oligomeric band was observed, suggesting LHCSR1 in a dimeric form in *Nicotiana* thylakoid membranes as previously reported for PSBS in plants (39). Considering all the fraction containing PpLHCSR1, the estimated yield (in Chl) of the recombinant protein is 0.13% and 0.03% in *N. benthamiana* and *N. tabacum* respectively. HPLC analysis on eluted slices showed that fractions enriched in PpLHCSR1 protein were characterized by a very high Chl *a/b* ratio, with values comprised between 8 and 24 (Fig. 6C & D), suggesting that PpLHCSR1 could bind Chl *b* in sub-stoichiometric amount only as previously reported also for *C. reinhardtii* LHCSR3 proteins (20) and native LHCSR1 from *P. patens* (22).

Absorption spectra of LHCSR-enriched and LHCb-enriched fractions were shown in Fig. 7 A-C. In the case of *N. benthamiana*, the spectrum of the fraction eluted from the green gel and containing PpLHCSR1 protein was characterized by a Qy absorption peak red-shifted to 678.8 nm while the eluate from corresponding area of the gel in WT lane only exhibited a weak and unresolved spectrum (Fig. 7A). Also in *N. tabacum* the eluted fraction containing PpLHCSR1 protein was

characterized by a Qy absorption peak red-shifted to 676.6 nm vs 674.4 nm of the corresponding area of the gel in WT lane (Fig. 7B), closely featuring the native spectrum of LHCSR of *P. patens* (22) (Fig. 7C).

Isolation of LHCSR1 using membrane fractionation and sucrose gradient ultracentrifugation—As an alternative approach to the isolation of recombinant PpLHCSR1, we fractionated stacked thylakoid membranes with α -DM (0.6%, 0.8%, 1%) to obtain a supernatant fraction (S) enriched in stroma membrane proteins and a pellet (P) containing grana partitions in both systems. Pellet yield was between 40 and 70% of Chl depending on detergent concentration. The Chl *a/b* was also in agreement with the Chl yield showing a Chl *a/b* decrease in the P by increasing the detergent concentration while the Chl *a/b* of the S was the specular image of Chl *a/b* of P (Table 1). Immunoblotting of the P vs S fractions showed that grana obtained with the highest concentration of detergent were depleted of LHCSR1; this reflected the finding that LHCSR1 is localized in stroma-exposed membranes in *P. patens* (Pinnola et al. submitted). At 0.8% almost all LHCSR1 protein was in S fraction which yielded 52% and 41% of Chl in *N. benthamiana* and *N. tabacum*, respectively (Fig. 8A). The S fraction from WT and oeLHCSR1 of both plant systems were fractionated by sucrose gradient ultracentrifugation (0.05 to 0.8 M Sucrose). Results (Fig. 8B) showed that three bands were obtained from WT, the upper, yellowish, containing free pigments (B1), the second, with monomeric LHCs (B2), the third (B3) with trimeric LHCII. In the case of *N. benthamiana* (Fig. 8B on the left), the sample from oeLHCSR1 plants, contained two additional bands, one just above B2 (called B1-2) and one half way between B2 and B3 (called B2-3). Instead, in the case of *N. tabacum* only one additional band (B1-2), just above B2, was found (Fig. 8B on the right). Bands were carefully harvested with a syringe and analyzed by SDS-PAGE and absorption spectra (Fig. 8C & D). Coomassie staining showed that both the additional bands (B1-2 and B2-3) in *N. benthamiana* and the B1-2 band in *N. tabacum* contained a ~23 KDa Coomassie-stained band with low levels of contaminants (Fig. 8C upper

panel) reactive to the α -PpLHCSR antibody (Fig. 8C underneath panel). Absorption spectra were very similar for B1-2 of both *N. tabacum* and *N. benthamiana* with the red-shifted peak at 678.3 nm and 678.8 nm (Fig. 8D). A similar spectrum was found for the lower LHCSR1 band (B2-3) of *N. benthamiana* which peaked at 679.4 nm, suggesting it contained an homodimeric LHCSR1 form. The lower level of B1-2 and the absence of B2-3 in *N. tabacum* could be related to the lower level of expression in this material. Anyway, considering the high biomass yield of *N. tabacum* plants, despite the low amount of LHCSR1 protein, we also tried to improve the purification level of PpLHCSR1 untagged version using *N. tabacum* plants. For this purpose, we applied a washing step of thylakoids with 1M NaBr to remove CF₁-ATPase (40) before the solubilization step. After the first sucrose gradient, the band containing LHCSR1 in monomeric form was loaded onto a second sucrose gradient in order to improve the purification and exclude the free pigments contamination (Fig. 9A). Coomassie staining showed that PpLHCSR1 untagged version did not contain other contamination and migrated shortly below PpLHCSR1 HisTag in SDS-PAGE (Fig. 9B). Absorption spectra of the two versions of the protein were very similar, suggesting the Histidine tag did not influence Car or Chl binding to the protein (Fig. 9C). Pigment binding was analyzed by HPLC and fitting the acetone extracts with the spectra of purified pigments (28, 29) (Table 2). Both the version of the protein were characterized by an high Chl *a/b* ratio, the pigment-protein bound mainly Chl *a*, trace amounts of Chl *b*, lutein (lut) and violaxanthin (viola).

In order to estimate the number of Chl bound to LHCSR we exploited the knowledge from LHCII crystal structure showing 14 Chl per polypeptide (41) as a reference for stoichiometric analysis of the pigment to protein ratio. For this purpose, various dilutions (0.6, 0.3, 0.15, 0.075 μ g Chl) of trimeric LHCII harvested from sucrose gradient and LHCSR1 isolated protein were loaded in a SDS-PAGE and stained with Coomassie blue (Fig. 10). We first verified the signal linearity for LHCII and LHCSR by densitometric analysis which was very high in all the samples analysed ($R^2 \geq 0.99$) (Fig. 10C & D). Since Coomassie dye binding depends on the basicity of a protein (number of

lysine, histidine and arginine residues) (42), we normalized the densitometric signal to the basic amino acid content. We found that 6.29 ± 0.41 Chl and 6.67 ± 0.28 Chl were bound to LHCSR1 with and without HisTag respectively.

Correlation between LHCSR1 accumulation and NPQ kinetics—We further proceeded to verify whether PpLHCSR1 protein was active in catalysing NPQ in the heterologous tobacco expression system. Leaves from *N. tabacum* plants expressing different levels of LHCSR1 were analysed for their NPQ kinetics as compared to WT ones lacking LHCSR1. WT leaf disks scored a NPQ activity of 1.97 upon 5 minutes of actinic light. oeLHCSR1 plants exhibited a somewhat higher NPQ than WT up to a value of 2.5 (Fig. 11A). In order to verify if a correlation could be found between the LHCSR1 expression level and NPQ, we plotted LHCSR1 amount vs NPQ max at 5 min in plants expressing PpLHCSR1 to different levels (Fig. 11B). A positive correlation, with a $R^2 \geq 0.96$, was found between NPQ and PpLHCSR1 level. The same procedure could not be performed for *N. benthamiana* because of high variability of results on the infected leaves subjected to a mechanical stress due to the agro-infiltration.

DISCUSSION

Heterologous expression systems for functional membrane proteins have been previously reported based on bacteria, cyanobacteria and yeasts (43, 44). However, the case of pigment-binding proteins of the LHC family is more complex due to the need for multiple chromophores essential for the folding of the holoprotein. Some chlorophyll-binding proteins, such as CP43, are able to fold only in the presence of Chl *a* (45) while LHCs require also Chl *b* and xanthophylls (46–49). This restricts the possible expression platforms to green algae and plants when aiming to the expression of active holocomplexes (50). Alternatively, the production of holocomplex can be divided into two steps, the first consisting into expression of apoprotein in bacteria, followed by refolding *in vitro* with purified pigments (48, 51).

Here, the first approach, adopted to obtain folded and active recombinant protein, was the transient expression of *P. patens* LHCSR1 (PpLHCSR1) in *N. benthamiana* as a

fast-track option for suitability of the expression system for different DNA constructs before moving to higher throughput expression systems (52). In a second stage, a stable expression system in *N. tabacum* was developed. Indeed, *N. tabacum* has been reported to be a major tool for molecular farming and offers several practical advantages over other systems. Both systems contain chromophores needed for LHCSR1 protein folding according to the biochemical analysis of holoproteins (20, 22) and yielded very similar pigment-protein complexes. The highest protein level was obtained with the transient expression of PpLHCSR1 in *N. benthamiana* at 4 dpi. This yielded 0.13 ± 0.025 mg Chl of LHCSR1 per 1 mg of Chl vs 0.036 ± 0.002 mg of Chl of thylakoids obtained from stably transformed *N. tabacum* (Fig. 5A). However, this gap is likely to be decreased when stably transformed plants, presently at the T2 generation, will reach homozygosis upon self-crossing. In the case of PpLHCSR1 HisTag, the amount of the protein was even lower, namely 0.021 ± 0.001 and 0.011 ± 0.003 mg of Chl, respectively per 1 mg of Chl of thylakoids in *N. benthamiana* and *N. tabacum* (Fig. 5B).

The heterologous protein was correctly addressed to thylakoid membranes and processed to an apparent MW indistinguishable from that observed in SDS-PAGE of moss thylakoids, strongly suggesting a correct targeting and processing of the pre-protein encoded by the constructs. In addition, the fractionation of thylakoid membrane domains showed PpLHCSR1 is located in stroma-exposed membranes, including grana margins which are solubilized by the α -DM treatment (53). This is in agreement with the localization of LHCSR1 in *P. patens* (Pinnola et al. submitted), implying that the protein elements, although unknown, that determine the partition of this LHC protein family member in the stroma membranes are acting in both *Physcomitrella* and *Nicotiana*. It should be noted, in fact, that most LHC proteins are located in grana membranes in plants unless are tightly bound to PSI (54). Rather, LHCSR1 appears not to be part of a permanently assembled supercomplex since it is found as a low MW pigment protein in sucrose gradient upon solubilization with the mild detergent α -DM (Fig. 2 & 8).

The aggregation state of recombinant PpLHCSR1 expressed in *Nicotiana* heterologous systems was mostly monomeric as judged from mobility upon ultracentrifugation and in non-denaturing green gels (Fig. 2 & 6). Nevertheless, higher MW forms of PpLHCSR1 were detected with lower mobility in green gels from both *N. benthamiana* and *N. tabacum* (Fig. 6A & B). Upon loading the sample in a lower density sucrose gradient (0.05-0.8 M sucrose) and with longer ultracentrifugation time, a LHCSR1-band was observed from both expression systems running at higher apparent MW than monomeric LHCs (Fig. 8B). It can be asked whether this corresponded to homo- or hetero-oligomer. First, we observed that the oligomeric form migrated slower than monomeric LHCs band but faster than LHCII trimers in Deriphat-PAGE and, conversely, faster than monomeric LHCs but slower than PSI in sucrose gradient. This is consistent with a dimer, although a trimeric aggregation state cannot entirely be excluded since the monomeric LHCSR1 is somehow smaller than monomeric LHCs (Fig. 2A, 6 A-B and 8 B). In the case of *N. benthamiana*, absorption spectra of the two bands from gradient (Fig. 8D) are very similar if not identical, allowing for the effect of minor contaminations. Since all other LHCs bind Chl *b* and are blue-shifted in the absorption peak, heterodimerization would likely lead to a change in the spectra. Together with the presence of only very minor contaminations in SDS-PAGE gels (Fig. 8C) this suggests the most likely state of LHCSR1 is an homodimer. LHC proteins can be found as trimers (LHCII), monomers (CP29, CP26, CP24) and dimers (LHCAs) (55–57). For both the Lhc-like proteins involved in NPQ triggering, namely PSBS and LHCSR3 from *Chlamydomonas*, there have been reports of dimeric organization, although in most conditions the most abundant form was a monomer (20, 22, 39). In this respect the recombinant LHCSR1 purified from *Nicotiana* closely features the properties of the homologous systems.

The different purification methods that we used in this work were consistent in yielding a pigment protein highly enriched in Chl *a*, with a red-shifted peak in the Qy range (679.1 nm), consistently with previous reports on recombinant *C. reinhardtii* LHCSR3 refolded *in vitro* (20, 23) or purified from *P. patens* (22).

The most pure preparation obtained, although in small amounts, had an exceedingly high Chl *a/b* ratio (Table 2). Based on a stoichiometry of 7 Chl per polypeptide (20), only 1 LHCSR molecule in 12 actually binds a Chl *b* chromophore. The most likely interpretation is that LHCSR1 binds Chl *a* only and that the traces of Chl *b* comes from contaminations, although undetectable in SDS-PAGE. This result is in contrast with previous reports on *C. reinhardtii* LHCSR3 obtained from refolding *in vitro* with pigments which has a Chl *a/b* ratio of 7 (20, 23), suggesting that conditions during biogenesis of LHCSR *in vivo* are more stringent than refolding *in vitro* as for pigment selectivity, in agreement with previous reports (48, 58). This is the first member of the LHC family which binds Chl *a* as the only porphyrin so far reported and is consistent with the accumulation of LHCSR3 in the Chl *b*-less *Cbs3* strain of *C. reinhardtii* (20). The alternative hypothesis that Chl *b* is bound to LHCSR1 *in vivo* but is lost during purification cannot be excluded, in principle. In this case different purification procedures would yield LHCSR1 preparation with different Chl *b* content. Yet, LHCSR1 purified by single step Deriphat-PAGE (Fig. 6) only binds Chl *b* in traces as His-tag LHCSR1 whose purification involves repeated washing with detergent solutions (Fig. 4). Chl *b* is needed for folding of most LHCs (46) and can replace Chl *a* in most sites (58) yielding stable complexes. X-ray analysis of LHCII revealed that Chl *b* is involved in a network of H-bonds involving carbonyl group at position C7 which stabilizes the structure of the pigment-protein (41). Among LHC proteins, the Chl *b*-rich LHCII complex exhibits essentially a single 3.6 ns fluorescence lifetime while decays kinetics from the Chl *a*-rich CP29 reveals at least three lifetimes, the amplitude of the shortest ones being increased upon zeaxanthin binding to site L2 (59). We suggest that the absence of Chl *b* might be important in easing the switching of LHCSR1 from unquenched to quenched conformation upon lumen acidification (20) and zeaxanthin binding (22). Besides Chl *a*, lutein and violaxanthin were found in very similar amounts, assuming that antheraxanthin (in traces) is bound to the same site(s) (likely site L2) as violaxanthin. With a Chl/Car ratio of 2.32 determined for LHCSR1 without HisTag, the minimal hypothesis, is of 2 xanthophylls and 4

Chl. However, we obtained a 6.7 ± 0.29 Chl per LHCSR polypeptide ratio by Coomassie-binding which is half the chromophore complement of any other LHC protein so far reported upon crystallization (41, 60, 61). A consensus figure of 4 xanthophylls ± 1 and 8 Chl ± 1 is a likely possibility since up to 4 xanthophyll binding sites have been reported (41). In either case the number of Chl of LHCSR1 is well below that of LHCII and CP29, consistent with the low level of sequence conservation between LHCII and LHCSR1 (24% identity, 37% similarity). It should be noticed that PSBS, a member of the LHC family involved in energy dissipation does not exhibit Chl binding sites (15) and sequence identity with LHCII is 20,8%.

Structure/function studies require the protein is functional. Indeed, the expression of recombinant PpLHCSR1 increased the high light-induced quenching activity in *N. tabacum* from 2 to 2.7 (Fig. 11A). It should be noted that WT *N. tabacum* is active in NPQ from resident PSBS. We therefore expected a background NPQ activity and a further increase in NPQ amplitude in oeLHCSR1 plants if the protein was active. The correlation of NPQ activity elicited by 5 minutes high light treatment with the accumulation level of LHCSR1 was very good ($R^2 \geq 0.96$), intercepting the 0 LHCSR1 protein line at $\text{NPQ} = 1.97$, i.e. the level of activity found in WT leaves. In the case of *N. benthamiana*, we could not directly prove the quenching activity of LHCSR1 transiently expressed, because of the high variability of NPQ activity likely induced by the infiltration procedure. Indeed, a strong down-regulation of PSII quantum yield has been reported upon *A. tumefaciens* infection (62). However, the identical spectra of the protein preparations from *N. tabacum* and *N. benthamiana* and the same localization of LHCSR1 in stroma-exposed

membranes strongly suggest both expression systems yield into the same preparation.

In this work we have obtained purification of PpLHCSR1 by (i) Ni^{++} -ion affinity chromatography (Fig. 4), (ii) non-denaturing Deriphat-PAGE (Fig. 6) or (iii) membrane fractionation followed by sucrose gradient ultracentrifugation (Fig. 8 & 9). We did not succeed in purification by ion-exchange chromatography and preparative IEF because of heavy co-fractionation with contaminants (not shown). The best purity was obtained by affinity chromatography (Fig. 4). Nevertheless, the low level of accumulation in thylakoids of the PpLHCSR1 HisTag makes the final yield low (1/1000) on a Chl basis. Better yield were obtained using untagged versions of the constructs corresponding to 5/1000 and 9/1000, based on Chl molar ratios, for *N. tabacum* and *N. benthamiana*, respectively.

We conclude that heterologous expression of PpLHCSR1 in *Nicotiana* yielded an active protein which has properties similar, if not identical, to those of LHCSR1 purified from the homologous system *P. patens* and is suitable for the study of molecular basis of NPQ in algae and mosses with the further advantage that a single gene product rather than a mixture of two (LHCSR1+LHCSR2) was obtained. Further studies are needed in order to understand the reasons for the lower specific NPQ activity in *Nicotiana* vs *Physcomitrella*. Likely the localization of the protein is the stroma membranes of thylakoids which is rich in LHCII in mosses but not in plants (Pinnola et al. PhD thesis, 2014) thus allowing for quenching of a small fraction only of highly fluorescent LHCII in plants.

Acknowledgements. We like to thank Matteo Ballottari for helpful discussion. Research was funded in part through the European Union Seventh Framework Programme for Research Project 316427, Environmental Acclimation of Photosynthesis; the Italian Ministry of Agriculture, Food and Forestry Project HYDROBIO.

Conflict of interest: The authors declare that they have no conflicts of interest with the contents of this article.

Author contributions: AP performed the stable transformation of *N. tabacum*; LG and AA performed the transient expression of *N. benthamiana*; MM, LA, EG and MP provided technology

and supervised the transformation and plant regeneration procedures; AP, LG and SC purified and characterized the protein; SC performed HPLC pigment analysis and helped with data analysis. AP wrote the manuscript. RB designed the study, supervised the work and revised the manuscript.

REFERENCES

1. Barber, J., and Andersson, B. (1992) Too much of a good thing: light can be bad for photosynthesis. *Trends Biochem. Sci.* **17**, 61–6
2. Miller, G., Shulaev, V., and Mittler, R. (2008) Reactive oxygen signaling and abiotic stress. *Physiol. Plant.* **133**, 481–9
3. Takahashi, S., and Murata, N. (2008) How do environmental stresses accelerate photoinhibition? *Trends Plant Sci.* **13**, 178–82
4. Genty, B., Briantais, J. M., and Baker, N. R. (1989) The relationship between the quantum yield of photosynthetic electron transport and quenching of chlorophyll fluorescence. *iochimica Biophys. Acta.* **990**, 87–92
5. Niyogi, K. K. (2000) Safety valves for photosynthesis. *Curr. Opin. Plant Biol.* **3**, 455–60
6. Külheim, C., Agren, J., and Jansson, S. (2002) Rapid regulation of light harvesting and plant fitness in the field. *Science.* **297**, 91–3
7. Nilkens, M., Kress, E., Lambrev, P., Miloslavina, Y., Müller, M., Holzwarth, A. R., and Jahns, P. (2010) Identification of a slowly inducible zeaxanthin-dependent component of non-photochemical quenching of chlorophyll fluorescence generated under steady-state conditions in Arabidopsis. *Biochim. Biophys. Acta.* **1797**, 466–75
8. Dall'Osto, L., Caffarri, S., and Bassi, R. (2005) A mechanism of nonphotochemical energy dissipation, independent from PsbS, revealed by a conformational change in the antenna protein CP26. *Plant Cell.* **17**, 1217–32
9. Powles, S. B., and Björkman, O. (1982) Photoinhibition of photosynthesis: effect on chlorophyll fluorescence at 77K in intact leaves and in chloroplast membranes of Nerium oleander. *Planta.* **156**, 97–107
10. Bruce, D., Samson, G., and Carpenter, C. (1997) The origins of nonphotochemical quenching of chlorophyll fluorescence in photosynthesis. Direct quenching by P680+ in photosystem II enriched membranes at low pH. *Biochemistry.* **36**, 749–55
11. Cazzaniga, S., Dall' Osto, L., Kong, S.-G., Wada, M., and Bassi, R. (2013) Interaction between avoidance of photon absorption, excess energy dissipation and zeaxanthin synthesis against photooxidative stress in Arabidopsis. *Plant J.* **76**, 568–79
12. Duysens, L., and Sweers, H. (1963) Mechanism of two photo- chemical reactions in algae as studied by means of fluorescence. *Stud. Microalgae Photosynth. Bact. (special issue Plant Cell Physiol)*

13. Li, X. P., Björkman, O., Shih, C., Grossman, A. R., Rosenquist, M., Jansson, S., and Niyogi, K. K. (2000) A pigment-binding protein essential for regulation of photosynthetic light harvesting. *Nature*. **403**, 391–5
14. Peers, G., Truong, T. B., Ostendorf, E., Busch, A., Elrad, D., Grossman, A. R., Hippler, M., and Niyogi, K. K. (2009) An ancient light-harvesting protein is critical for the regulation of algal photosynthesis. *Nature*. **462**, 518–21
15. Dominici, P., Caffarri, S., Armenante, F., Ceoldo, S., Crimi, M., and Bassi, R. (2002) Biochemical properties of the PsbS subunit of photosystem II either purified from chloroplast or recombinant. *J. Biol. Chem.* **277**, 22750–8
16. Bonente, G., Howes, B. D., Caffarri, S., Smulevich, G., and Bassi, R. (2008) Interactions between the photosystem II subunit PsbS and xanthophylls studied in vivo and in vitro. *J. Biol. Chem.* **283**, 8434–45
17. Ahn, T. K., Avenson, T. J., Ballottari, M., Cheng, Y.-C., Niyogi, K. K., Bassi, R., and Fleming, G. R. (2008) Architecture of a charge-transfer state regulating light harvesting in a plant antenna protein. *Science*. **320**, 794–7
18. Avenson, T. J., Ahn, T. K., Zigmantas, D., Niyogi, K. K., Li, Z., Ballottari, M., Bassi, R., and Fleming, G. R. (2008) Zeaxanthin radical cation formation in minor light-harvesting complexes of higher plant antenna. *J. Biol. Chem.* **283**, 3550–8
19. Dall'Osto, L., Holt, N. E., Kaligotla, S., Fuciman, M., Cazzaniga, S., Carbonera, D., Frank, H. A., Alric, J., and Bassi, R. (2012) Zeaxanthin protects plant photosynthesis by modulating chlorophyll triplet yield in specific light-harvesting antenna subunits. *J. Biol. Chem.* 10.1074/jbc.M112.405498
20. Bonente, G., Ballottari, M., Truong, T. B., Morosinotto, T., Ahn, T. K., Fleming, G. R., Niyogi, K. K., and Bassi, R. (2011) Analysis of LhcSR3, a protein essential for feedback de-excitation in the green alga *Chlamydomonas reinhardtii*. *PLoS Biol.* **9**, e1000577
21. Alboresi, A., Gerotto, C., Giacometti, G. M., Bassi, R., and Morosinotto, T. (2010) Physcomitrella patens mutants affected on heat dissipation clarify the evolution of photoprotection mechanisms upon land colonization. *Proc. Natl. Acad. Sci. U. S. A.* **107**, 11128–33
22. Pinnola, A., Dall'Osto, L., Gerotto, C., Morosinotto, T., Bassi, R., and Alboresi, A. (2013) Zeaxanthin Binds to Light-Harvesting Complex Stress-Related Protein to Enhance Nonphotochemical Quenching in Physcomitrella patens. *Plant Cell*. **25**, 3519–34
23. Liguori, N., Roy, L. M., Opacic, M., Durand, G., and Croce, R. (2013) Regulation of Light Harvesting in the Green Alga *Chlamydomonas reinhardtii*: The C-Terminus of LHCSR Is the Knob of a Dimmer Switch. *J. Am. Chem. Soc.* **135**, 18339–42
24. Karimi, M., Inzé, D., and Depicker, A. (2002) GATEWAY vectors for Agrobacterium-mediated plant transformation. *Trends Plant Sci.* **7**, 193–5

25. Horsch, R. B., Klee, H. J., Stachel, S., Winans, S. C., Nester, E. W., Rogers, S. G., and Fraley, R. T. (1986) Analysis of *Agrobacterium tumefaciens* virulence mutants in leaf discs. *Proc. Natl. Acad. Sci. U. S. A.* **83**, 2571–5
26. Bassi, R., and Simpson, D. J. (1987) Chlorophyll-proteins of barley photosystem I. *Eur. J. Biochem.*
27. Peter, G. F., Takeuchi, T., and Philip Thornber, J. (1991) Solubilization and two-dimensional electrophoretic procedures for studying the organization and composition of photosynthetic membrane polypeptides. *Methods.* **3**, 115–124
28. Gilmore, A. M., and Yamamoto, H. Y. (1991) Zeaxanthin Formation and Energy-Dependent Fluorescence Quenching in Pea Chloroplasts under Artificially Mediated Linear and Cyclic Electron Transport. *Plant Physiol.* **96**, 635–43
29. Croce, R., Canino, G., Ros, F., and Bassi, R. (2002) Chromophore organization in the higher-plant photosystem II antenna protein CP26. *Biochemistry.* **41**, 7334–43
30. Laemmli, U. K. (1970) Cleavage of Structural Proteins during the Assembly of the Head of Bacteriophage T4. *Nature.* **227**, 680–685
31. Demmig-Adams, B., Gilmore, A. M., and Adams, W. W. (1996) Carotenoids 3: in vivo function of carotenoids in higher plants. *FASEB J.* **10**, 403–12
32. Fischer, R., and Emans, N. (2000) Molecular farming of pharmaceutical proteins. *Transgenic Res.* **9**, 279–99; discussion 277
33. Kapila, J., De Rycke, R., Van Montagu, M., and Angenon, G. (1997) An *Agrobacterium*-mediated transient gene expression system for intact leaves. *Plant Sci.* **122**, 101–108
34. Goodin, M. M., Zaitlin, D., Naidu, R. A., and Lommel, S. A. (2008) *Nicotiana benthamiana*: its history and future as a model for plant-pathogen interactions. *Mol. Plant. Microbe. Interact.* **21**, 1015–26
35. Krysan, P. J., Young, J. C., Jester, P. J., Monson, S., Copenhaver, G., Preuss, D., and Sussman, M. R. (2002) Characterization of T-DNA insertion sites in *Arabidopsis thaliana* and the implications for saturation mutagenesis. *OMICS.* **6**, 163–74
36. Stengel, A., Soll, J., and Bölder, B. (2007) Protein import into chloroplasts: new aspects of a well-known topic. *Biol. Chem.* **388**, 765–72
37. Hooper, J., and Eggink, L. (1999) Assembly of light-harvesting complex II and biogenesis of thylakoid membranes in chloroplasts. *Photosynth. Res.* **61**, 197–215
38. Dainese, P., and Bassi, R. (1991) Subunit stoichiometry of the chloroplast photosystem II antenna system and aggregation state of the component chlorophyll a/b binding proteins. *J. Biol. Chem.* **266**, 8136–42
39. Bergantino, E., Segalla, A., Brunetta, A., Teardo, E., Rigoni, F., Giacometti, G. M., and Szabò, I. (2003) Light- and pH-dependent structural changes in the PsbS subunit of photosystem II. *Proc. Natl. Acad. Sci. U. S. A.* **100**, 15265–70

40. Strotmann, H., Kleefeld, S., and Lohse, D. (1987) Control of ATP hydrolysis in chloroplasts. *FEBS Lett.* **221**, 265–269
41. Liu, Z., Yan, H., Wang, K., Kuang, T., Zhang, J., Gui, L., An, X., and Chang, W. (2004) Crystal structure of spinach major light-harvesting complex at 2.72 Å resolution. *Nature.* **428**, 287–92
42. Tal, M., Silberstein, A., and Nusser, E. (1985) Why does Coomassie Brilliant Blue R interact differently with different proteins? A partial answer. *J. Biol. Chem.* **260**, 9976–9980
43. Bernaudat, F., Frelet-Barrand, A., Pochon, N., Dementin, S., Hivin, P., Boutigny, S., Rioux, J.-B., Salvi, D., Seigneurin-Berny, D., Richaud, P., Joyard, J., Pignol, D., Sabaty, M., Desnos, T., Pebay-Peyroula, E., Darrouzet, E., Vernet, T., and Rolland, N. (2011) Heterologous expression of membrane proteins: choosing the appropriate host. *PLoS One.* **6**, e29191
44. Rosgaard, L., de Porcellinis, A. J., Jacobsen, J. H., Frigaard, N.-U., and Sakuragi, Y. (2012) Bioengineering of carbon fixation, biofuels, and biochemicals in cyanobacteria and plants. *J. Biotechnol.* **162**, 134–47
45. Ji Liu, Xie, S.-S., Yue Luo, Zhu, G.-F., and Du, L.-F. (2014) Soluble expression of Spinach psbC gene in Escherichia coli and in vitro reconstitution of CP43 coupled with chlorophyll a only. *Plant Physiol. Biochem.* **79**, 19–24
46. Plumley, F. G., and Schmidt, G. W. (1987) Reconstitution of chlorophyll a/b light-harvesting complexes: Xanthophyll-dependent assembly and energy transfer. *Proc. Natl. Acad. Sci. U. S. A.* **84**, 146–50
47. Havaux, M., Dall'Osto, L., and Bassi, R. (2007) Zeaxanthin has enhanced antioxidant capacity with respect to all other xanthophylls in Arabidopsis leaves and functions independent of binding to PSII antennae. *Plant Physiol.* **145**, 1506–20
48. Giuffra, E., Cugini, D., Croce, R., and Bassi, R. (1996) Reconstitution and Pigment-Binding Properties of Recombinant CP29. *Eur. J. Biochem.* **238**, 112–120
49. Croce, R., Weiss, S., and Bassi, R. (1999) Carotenoid-binding sites of the major light-harvesting complex II of higher plants. *J. Biol. Chem.* **274**, 29613–23
50. Flachmann, R., and Kühlbrandt, W. (1996) Crystallization and identification of an assembly defect of recombinant antenna complexes produced in transgenic tobacco plants. *Proc. Natl. Acad. Sci. U. S. A.* **93**, 14966–71
51. Paulsen, H., Finkenzeller, B., and Kühlein, N. (1993) Pigments induce folding of light-harvesting chlorophyll a/b-binding protein. *Eur. J. Biochem.* **215**, 809–16
52. Rycke, R. De, and Kapila, J. (1997) An agrobacterium-mediated transient gene expression intact leaves system for
53. Morosinotto, T., Segalla, A., Giacometti, G. M., and Bassi, R. (2010) Purification of structurally intact grana from plants thylakoids membranes. *J. Bioenerg. Biomembr.* **42**, 37–45
54. Simpson, D. J. (1983) Freeze-fracture studies on barley plastid membranes. VI. Location of the P700-chlorophyll a-protein 1. *Eur. J. Cell Biol.* **31**, 305–14

55. Dekker, J. P., and Boekema, E. J. (2005) Supramolecular organization of thylakoid membrane proteins in green plants. *Biochim. Biophys. Acta.* **1706**, 12–39
56. Wientjes, E., Oostergetel, G. T., Jansson, S., Boekema, E. J., and Croce, R. (2009) The role of Lhca complexes in the supramolecular organization of higher plant photosystem I. *J. Biol. Chem.* **284**, 7803–10
57. Ballottari, M., Girardon, J., Dall'Osto, L., and Bassi, R. (2012) Evolution and functional properties of photosystem II light harvesting complexes in eukaryotes. *Biochim. Biophys. Acta.* **1817**, 143–57
58. Croce, R., Müller, M. G., Bassi, R., and Holzwarth, A. R. (2003) Chlorophyll b to chlorophyll a energy transfer kinetics in the CP29 antenna complex: a comparative femtosecond absorption study between native and reconstituted proteins. *Biophys. J.* **84**, 2508–16
59. Moya, I., Silvestri, M., Vallon, O., Cinque, G., and Bassi, R. (2001) Time-resolved fluorescence analysis of the photosystem II antenna proteins in detergent micelles and liposomes. *Biochemistry.* **40**, 12552–61
60. Pan, X., Li, M., Wan, T., Wang, L., Jia, C., Hou, Z., Zhao, X., Zhang, J., and Chang, W. (2011) Structural insights into energy regulation of light-harvesting complex CP29 from spinach. *Nat. Struct. Mol. Biol.* **18**, 309–15
61. Ben-Shem, A., Frolow, F., and Nelson, N. (2003) Crystal structure of plant photosystem I. *Nature.* **426**, 630–5
62. Berger, S., Sinha, A. K., and Roitsch, T. (2007) Plant physiology meets phytopathology: plant primary metabolism and plant-pathogen interactions. *J. Exp. Bot.* **58**, 4019–26

FOOTNOTE

The abbreviations used are:

Car Carotenoids

Chl Chlorophyll

LHC Light Harvesting Complex

NPQ Non-Photochemical Quenching

PSII Photosystem II

α -DM n-Dodecyl- α -D-Maltopyranoside

oeLHCSR1 LHCSR1 over-expressing plants

oeLHCSR1 HisTag LHCSR1 with Histidine tail over-expressing plants

TABLE 1. Chlorophyll *a/b* ratio of supernatant and pellet fraction obtained solubilizing thylakoids of *N. tabacum* and *N. benthamiana* with different α -DM concentrations. Data are given as means \pm SD of at least three independent experiments.

TABLE 2. Pigment content, Chl *a/b* and Chl/Car ratio of purified LHCSR1 with and without HisTag. The individual pigment value was normalized to 8, the proposed number of Chl per polypeptide. **Car**, Carotenoids; **Chl**, Chlorophylls, **neo**, neoxanthin; **viola**, violaxanthin; **ante**, antheraxanthin; **lut**, lutein.

FIGURE 1. Expression analysis on *N. benthamiana* and *N. tabacum* transformation using two different PpLHCSR1 constructs and localization of PpLHCSR1 in thylakoid membranes of tobacco. A-D) Time-course PpLHCSR1 accumulation trial in *N. benthamiana* upon transient expression. Leaf disks collected daily post agro-infiltration (dpi) were ground in LB buffer, fractionated by SDS-PAGE and transferred on a PVDF membrane. Immunoblot analysis using a homemade α -PpLHCSR antibody of oeLHCSR1 (A) or oeLHCSR1 HisTag (B) are reported. Time course of LHCSR1 for oeLHCSR1 (C) or oeLHCSR1 HisTag (D). Data are presented as means \pm SD of three independent experiments. E-F) Immunoblot analysis on oeLHCSR1 (E) or oeLHCSR1 HisTag (B) plants of stably transformed *N. tabacum*. Antibody α -PpLHCSR was used. Equal volume for each leaf disks was loaded. Immuno-detection of α -CP43 antibody is shown as a control of equal loading. *P. patens* and *N. tabacum* WT thylakoids (1 μ g Chl) were loaded as positive and negative control, respectively. **Thyl.**, thylakoids; **Nb**, *N. benthamiana*; **Nt**, *N. tabacum*. G) Immunoblot analysis of thylakoid membranes purified from WT, oeLHCSR1 (oeSR1) and oeLHCSR1 HisTag (oeSR1 HisTag).

FIGURE 2. Fractionation of WT and oeLHCSR1 solubilized thylakoids of *N. benthamiana* and *N. tabacum*. A) Sucrose gradient of thylakoids solubilized with 0.8 % α -DM from WT and oeLHCSR1 of *N. benthamiana* and *N. tabacum* plants. B) Coomassie blue-stained SDS-PAGE analysis of green bands collected from sucrose gradient. An equal volume (50 μ l) of each band was loaded. A polypeptide corresponding to LHCSR1 molecular weight (MW), underlined in red, was clearly visible in band 1 (B1) and band 2 (B2) (corresponding to free pigments and monomeric LHCs respectively). C) Immunoblot analysis with α -PpLHCSR antibody. Thylakoids (**Thyl**) from oeLHCSR1 and WT were loaded as positive and negative control, respectively. B1, B2, B3 from WT thylakoids were loaded as additional negative control.

FIGURE 3. Absorption spectra of fractions obtained from sucrose gradient. A) Spectra of B1 fraction from WT (black line) vs oeLHCSR1 (gray line) of *N. benthamiana* and *N. tabacum* (B). C) Absorption spectra of B2 fraction from WT (black line) and oeLHCSR1 (gray line) of *N. benthamiana* and *N. tabacum* (D). Peak wavelengths are indicated.

FIGURE 4. PpLHCSR1 HisTag isolation and biochemical characterization. A) Absorption spectra of fraction eluted with 250 mM imidazole (gray line) after solubilization with α -DM of oeLHCSR1 HisTag thylakoids. The absorption spectrum of solubilized thylakoids (black line) is also reported. B) Coomassie-blue stained SDS-PAGE gel analysis of fractions eluted with different imidazole concentrations. Samples, containing 2 μ g of Chl, were loaded in each slot. Thylakoids (3 μ g of Chl) of WT, oeLHCSR1 HisTag (HT) of *N. tabacum* and WT of *P. patens* were also loaded as control. Immunoblot analysis using antibody α -PpLHCSR is shown in the panel below the gel. **Sol**, thylakoid solubilized; **FT**, flow through; **Thyl.**, thylakoids; **Nt**, *N. tabacum*; **Pp**, *P. patens* C) Sucrose gradient fractionation obtained by loading the fractions eluted from Ni^{++} column with 250 mM imidazole (on the left). Coomassie stain of SDS-PAGE of B2 and pellet (P) fractions (on the right). D) Absorption spectra of B1 (red line) and B2 (gray line) fractions from sucrose gradient. LHCII (black line) is reported for comparison.

FIGURE 5. Abundance of the recombinant PpLHCSR1 protein in the different expression systems. A) LHCSR1 immuno-titration on oeLHCSR1 thylakoids of *N. benthamiana* and *N. tabacum*. 0.125, 0.25, 0.5 and 0.75 μ g of Chl were loaded for each sample. In the case of LHCSR1HisTag purified protein, 0.012, 0.025 and 0.05 μ g of Chl were loaded. B) LHCSR1 immuno-titration on oeLHCSR1 HisTag thylakoids of *N. benthamiana* and *N. tabacum*. Filters were probed with α -PpLHCSR antibody.

FIGURE 6. PpLHCSR1 localization among pigment-binding complexes of *N. benthamiana* and *N. tabacum*. A-B) Non-denaturing gel electrophoresis of pigment-binding complexes from thylakoids of oeLHCSR1 and WT of *N. benthamiana* (A) and *N. tabacum* (B) after solubilization with 0.8% α -DM.

500 µg of Chl were loaded for each sample. C-D) Coomassie blue staining and immunoblotting analysis of the fractions eluted from the non-denaturing gel slices shown in (A & B) and separated in second dimension under denaturing conditions. The numbering of fractions reported on the top of the each filter corresponds to that of gel slices cut from the non-denaturing gel. A polypeptide corresponding to LHCSR1 molecular weight, underlined in red, was clearly visible in slices 5, 6 and 7 of oeLHCSR1 from both plant systems. Chlorophyll *a/b* ratio are indicated underneath each filter.

FIGURE 7. Spectroscopic analysis of recombinant PpLHCSR1 protein purified from Deriphat-PAGE. A) Absorption spectrum of slice 6 eluted from the gel. Sample containing PpLHCSR1 protein from oeLHCSR1 thylakoids (gray line) is compared with the corresponding fraction purified from *N. benthamiana* WT solubilized thylakoids (black line). B) Absorption spectrum of slice 6 eluted from the gel of *N. tabacum* thylakoids. Sample containing PpLHCSR1 protein from oeLHCSR1 thylakoids (gray line) compared to the corresponding fraction purified from WT (black line). C) Comparison among absorption spectra of fraction 6, containing LHCSR1 protein, from *N. benthamiana* (black line) and *N. tabacum* (light gray line) and native LHCSR from *P. patens* (dark gray line) isolated in Pinnola et al 2013.

FIGURE 8. Untagged PpLHCSR1 isolation and biochemical characterization. A) Immunoblot probed with α -PpLHCSR antibody of fractions obtained by solubilizing thylakoids by different concentration of α -DM. An equal amount of Chl (0.25 µg) was loaded for each fraction. Thylakoids of oeLHCSR1 of *N. benthamiana* and *N. tabacum* are shown as reference. **P**, pellet; **S**, supernatant **Thyl**, thylakoids; **Nb**, *N. benthamiana*; **Nt**, *N. tabacum*. B) Sucrose gradient of supernatant obtained solubilizing thylakoids with 0.8% α -DM from WT and oeLHCSR1 of both plant systems. C) Polypeptide composition of fractions harvested from sucrose gradient of oeLHCSR1 plants. 0.5 µg of Chl were loaded for B2, 0.3 µg of Chl for other green bands. In the underneath panel the immunoblot with α -PpLHCSR antibody is shown. D) Absorption spectra of monomeric LHCs (pink line) and B1-2 (black line) from sucrose gradient of *N. tabacum*, B1-2 (red line) and B2-3 (blue line) from sucrose gradient of *N. benthamiana*.

FIGURE 9. Purification of LHCSR1 without HisTag. A) Sucrose gradient of PpLHCSR1 enriched fraction. Enrichment was obtained by pooling the LHCSR-containing fractions from a first sucrose gradient (not shown). This second gradient allowed for separation of free pigments. B) Coomassie blue stained SDS-PAGE gels of fraction B2. LHCSR HisTag (LHCSR HT) was also loaded for reference. Loading was 0.3 µg Chl per lane. C) Absorption spectra of LHCSR1 with and without HisTag (gray and black lines, respectively).

FIGURE 10. Determination of Chl to polypeptide ratio in LHCSR1. A-B) Coomassie stained gels of various dilutions (0.6, 0.3, 0.15, 0.075 and 0.035 µg Chl) of LHCSR, LHCSR HisTag and LHCII (0.6, 0.3, 0.15 and 0.075 µg Chl). C) Plot of Coomassie stain vs chlorophyll amount for LHCII (upper panel) and LHCSR (underneath panel) showing linearity of the Coomassie binding). $R^2 \geq 0.99$. D) Plot of Coomassie stain vs chlorophyll amount for LHCII (upper panel) and LHCSR HisTag (underneath panel). $R^2 \geq 0.99$. The figure shows the result of a typical experiment.

FIGURE 11. Relation between NPQ activity and accumulation of PpLHCSR1 protein. A) NPQ kinetic measurements on *N. tabacum* leaf disks. *N. tabacum* samples expressing different level of PpLHCSR1 were compared to WT. B) Correlation between NPQ activity at the last light point (NPQ max) of *N. tabacum* plants and LHCSR accumulation. $R^2 \geq 0.96$. Data are presented as a means \pm SD ($n \geq 3$).

TABLE 1.

	Pellet				Supernatant		
	Thyl.	α -DM concentration (%)			α -DM concentration (%)		
		0.6	0.8	1	0.6	0.8	1
<i>N. benthamiana</i>	2.60 \pm 0.05	2.21 \pm 0.04	2.44 \pm 0.30	2.14 \pm 0.08	4.76 \pm 0.04	4.96 \pm 0.10	4.43 \pm 0.20
<i>N. tabacum</i>	2.54 \pm 0.06	2.48 \pm 0.02	2.29 \pm 0.02	2.11 \pm 0.03	4.64 \pm 0.05	4.73 \pm 0.10	4.22 \pm 0.30

TABLE 2.

	Chl <i>a</i> /Chl <i>b</i>	Chl/Car	Chl <i>a + b</i> normalization	pigment content						
				Chl <i>a</i>	Chl <i>b</i>	neo	viola	ante	lut	N° Car
LHCSR1 HisTag	37.94	2.02	8.00	7.79	0.21	0.00	1.83	0.09	2.04	3.96
LHCSR1	12.71	2.32	8.00	7.42	0.58	0.00	1.37	0.02	2.04	3.43

FIGURE 1

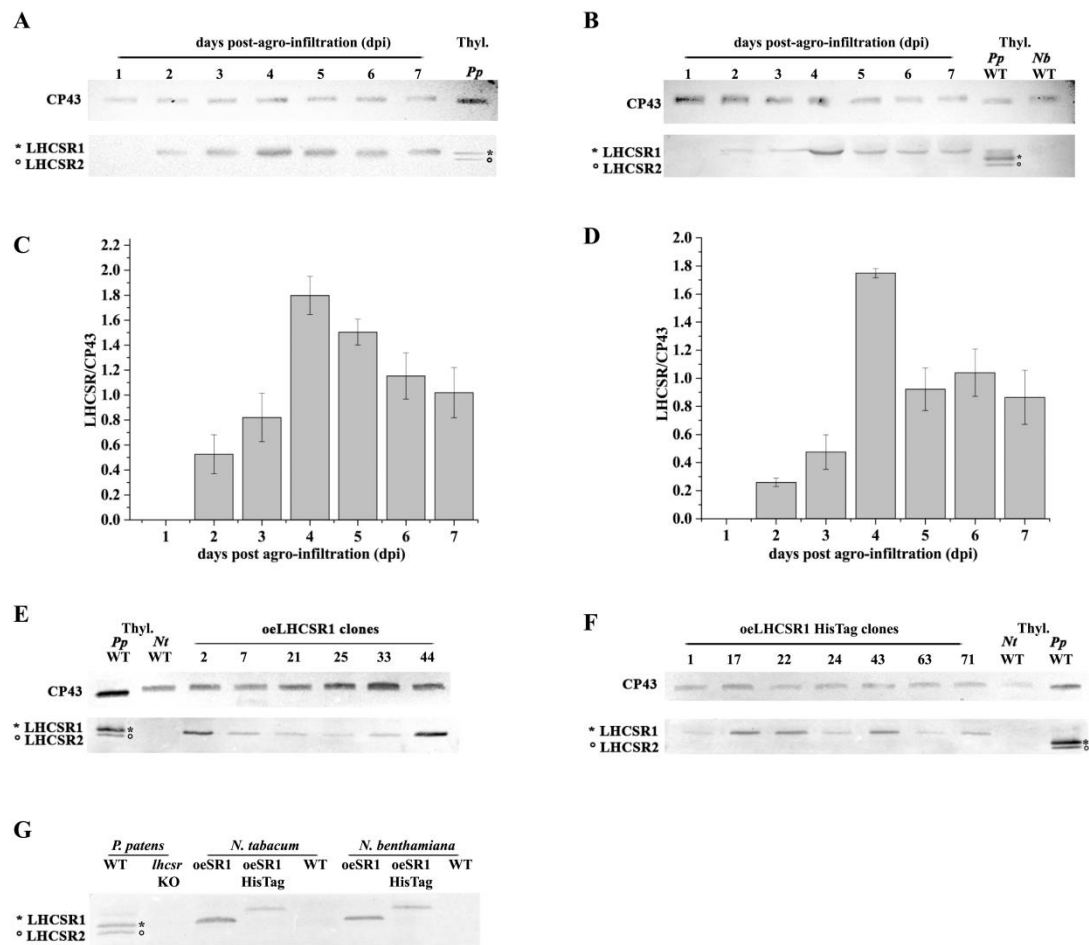


FIGURE 2

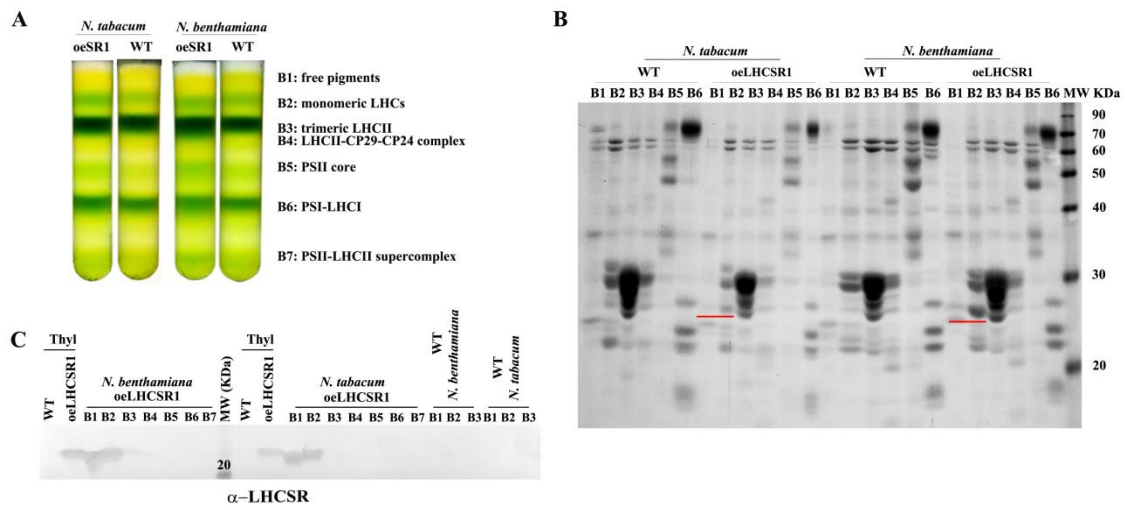


FIGURE 3

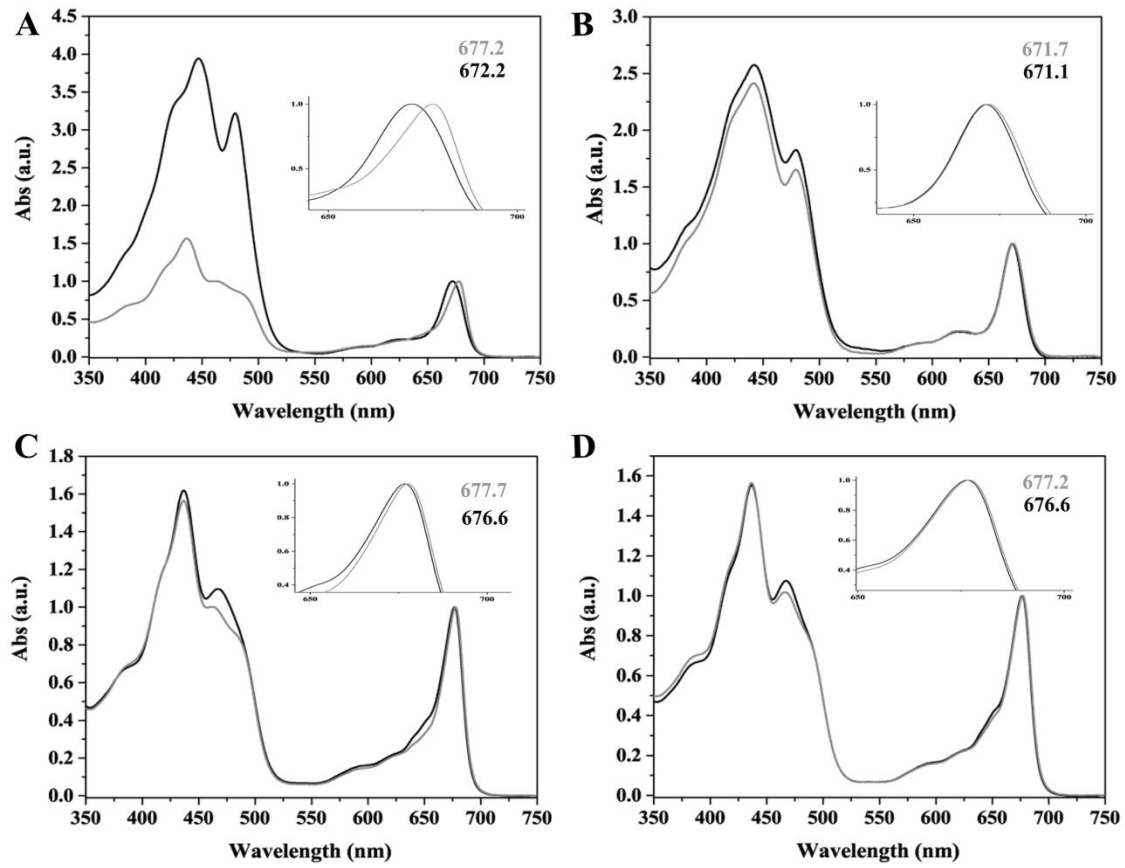


FIGURE 4

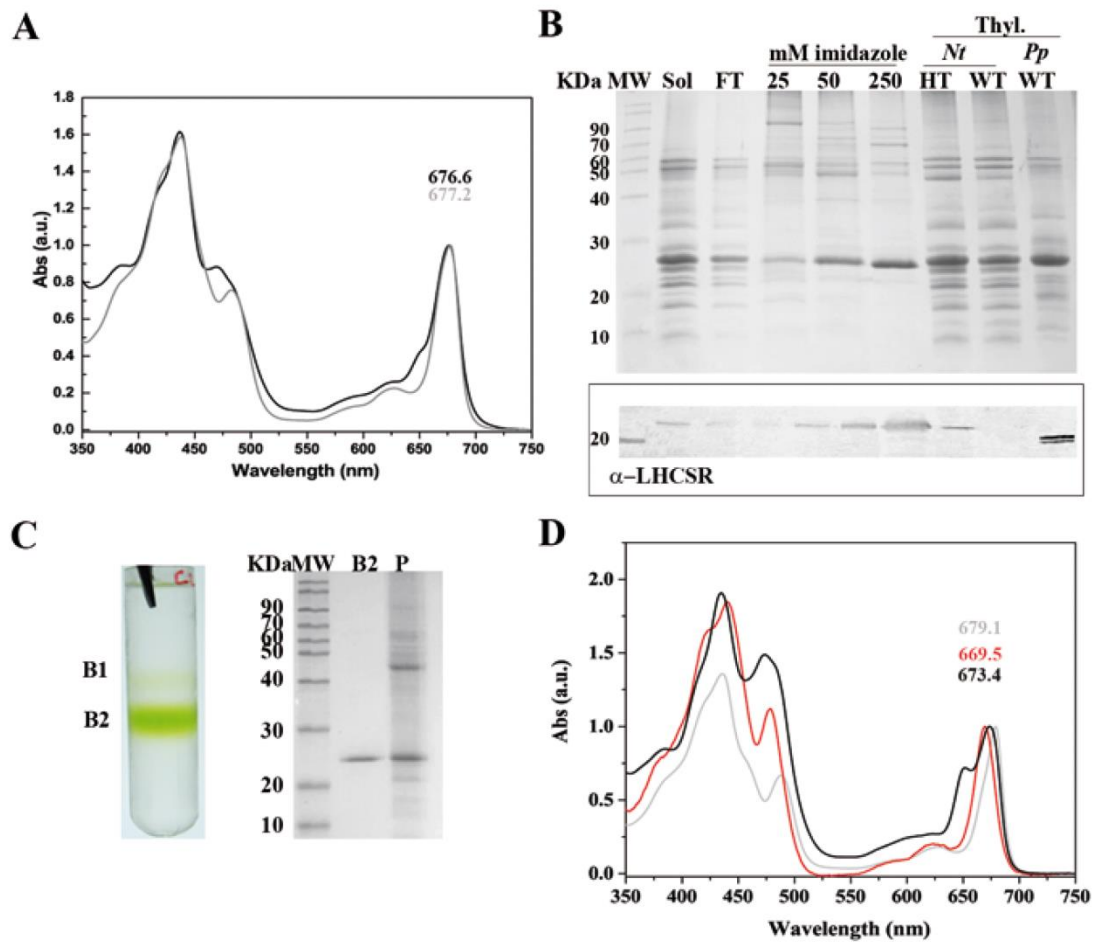


FIGURE 5

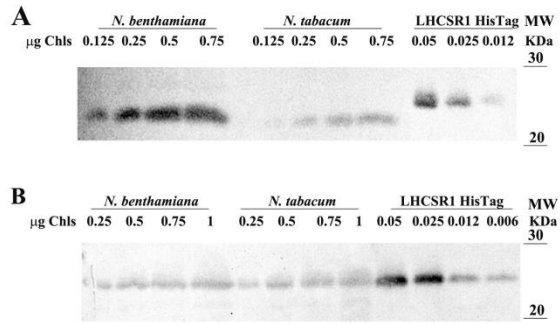


FIGURE 6

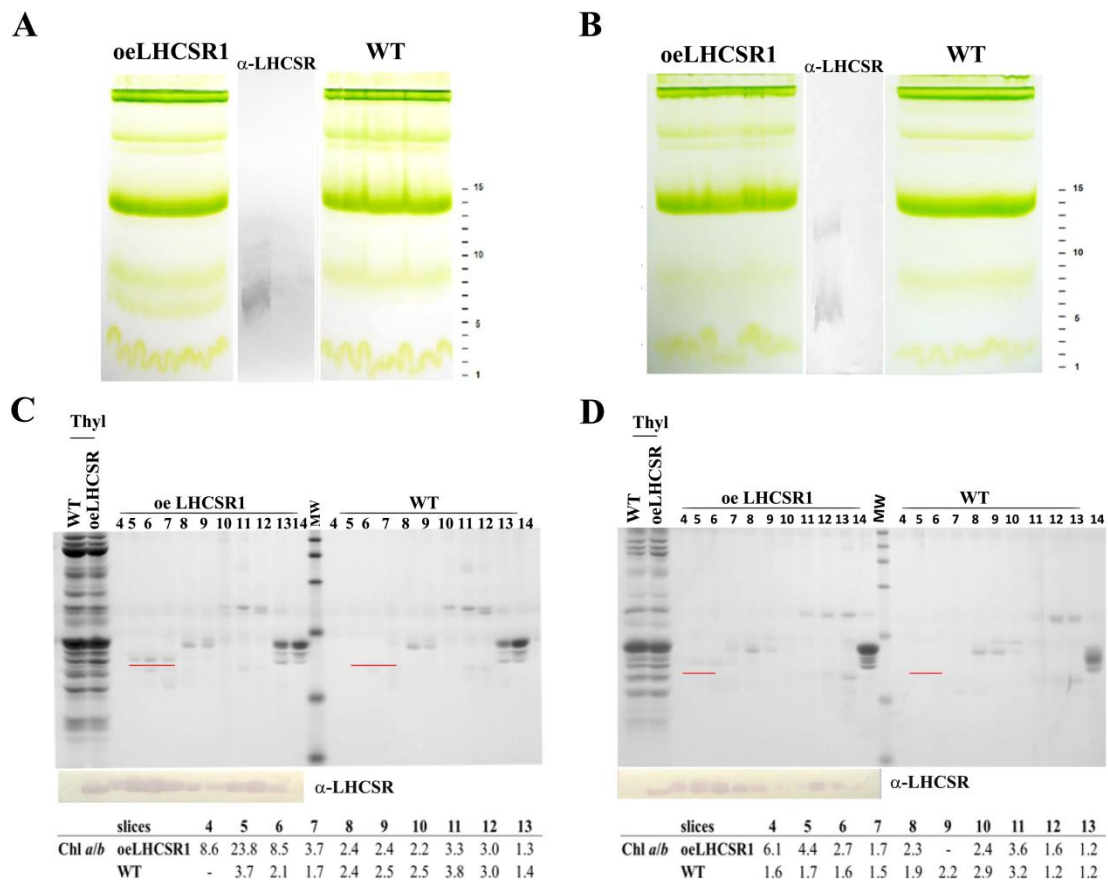


FIGURE 7

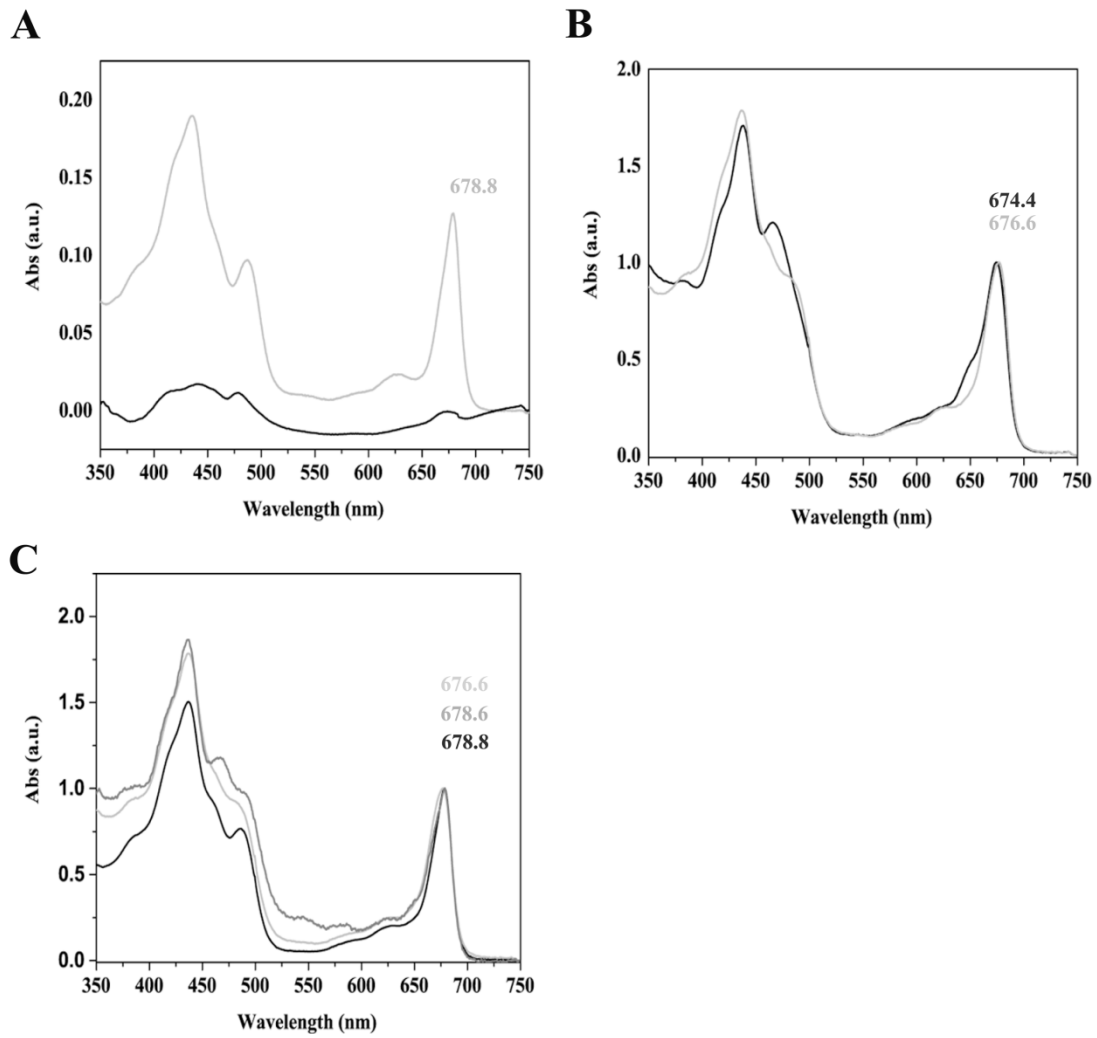


FIGURE 8

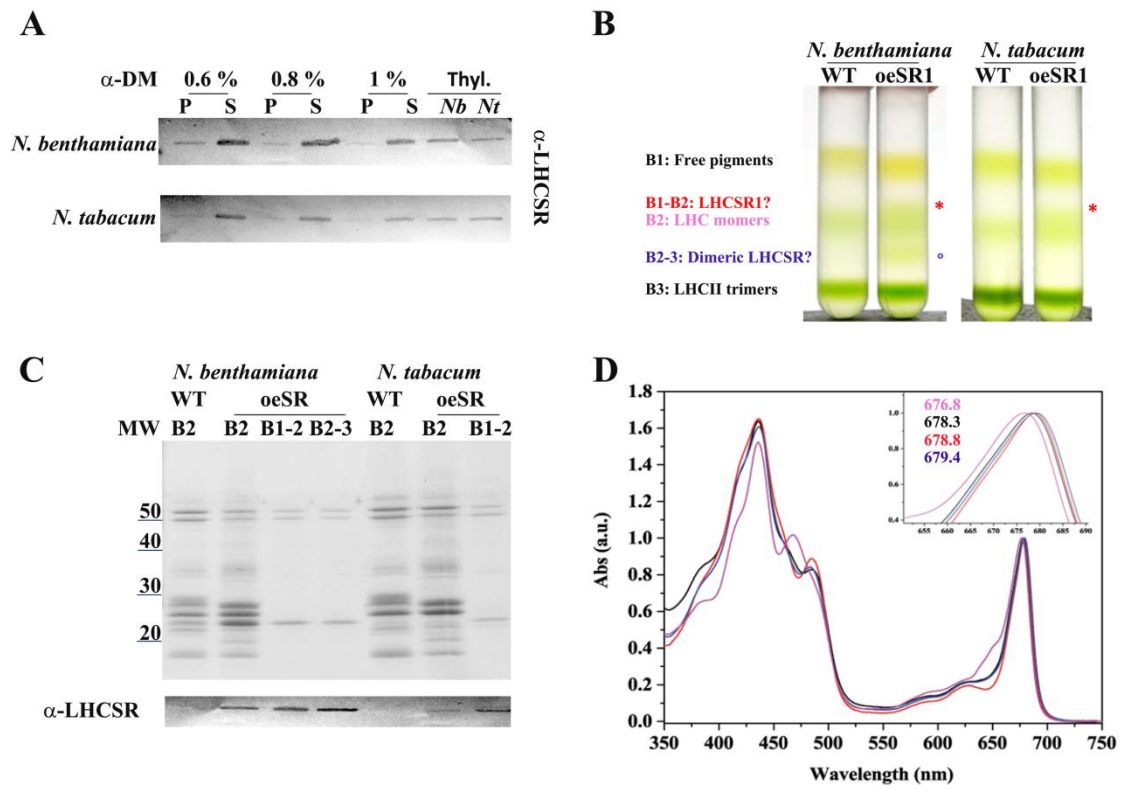


FIGURE 9

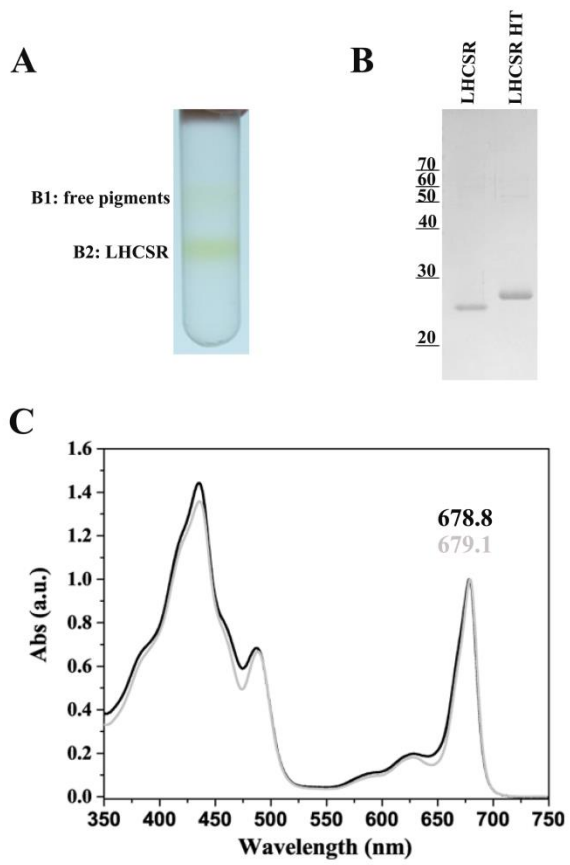


FIGURE 10

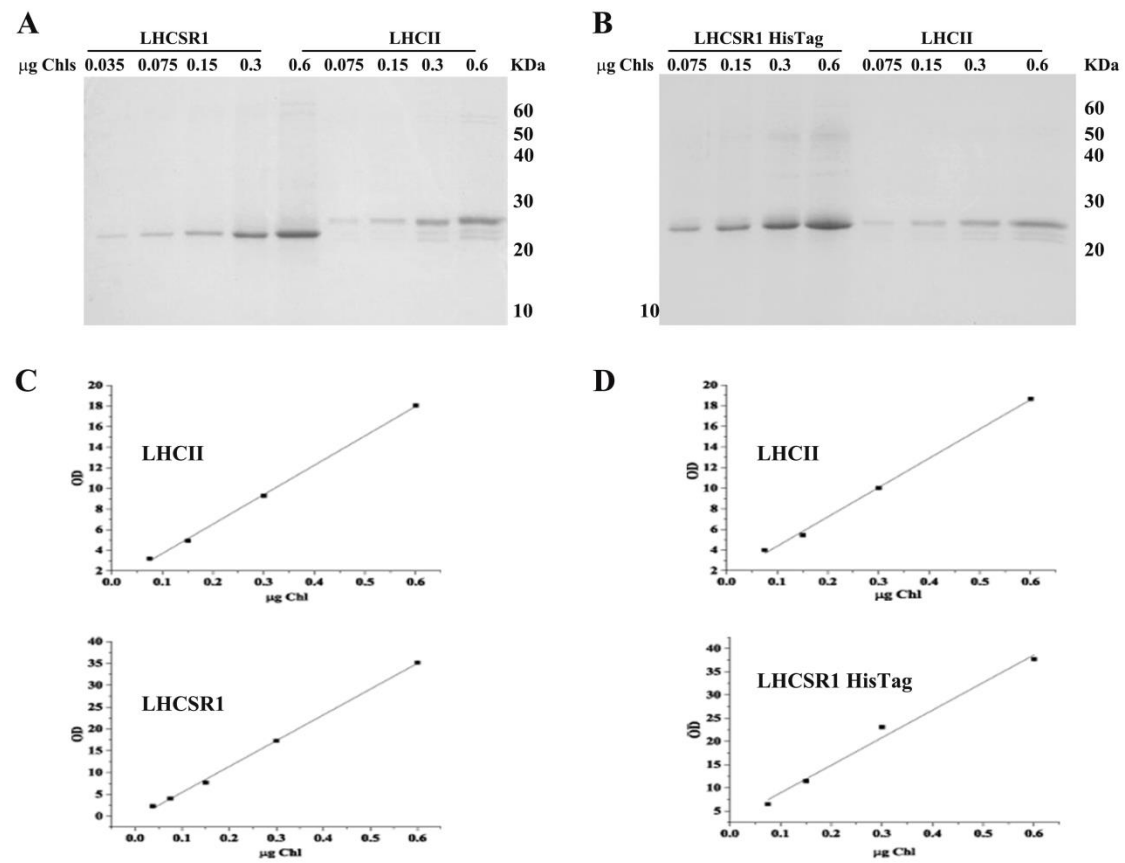


FIGURE 11

